

# Ab Initio Study of $\text{Li}_2\text{FeSO}$ Antiperovskite for Energy Storage

Zakaryaa Zarhri<sup>1\*</sup>

<sup>1</sup>CONAHCYT- Faculty of Chemical Sciences and Engineering, The Autonomous University of Morelos State, Av Universidad 1001, C.P. 62209, Cuernavaca, Morelos, Mexico.

**Abstract.** Density Functional Theory (DFT), in combination with the Wien2k software, is used to investigate the physical properties of  $\text{Li}_2\text{SO}$  antiperovskite modified by atomic substitution with Fe. The objective is to understand, at the electronic and molecular levels, the electrochemical behavior of the doped material and to optimize its performance. This research was conducted using the Linearized Augmented Plane Waves (LAPW) method for analyzing the electronic structure of the  $(\text{Li-Fe})_2\text{SO}$  antiperovskite. The density of states analysis reveals an improvement in the lithium storage capacity of the doped material, as well as in the stability and charge transport capacity of the electrode. Additionally, the presence of absorbance peaks at energies close to the energy levels of the lithium battery may indicate a high lithium storage capacity in the material, making it promising for battery applications.

## 1 Introduction

Energy storage is a topic of great importance in our times. Consequently, the study of some properties of lithium-ion batteries (LIBs) reveals a good energy density and low self-discharge [1], [2]. However, due to the current demand for higher storage capacity, greater energy density, safety, longer lifespan, and above all, lower costs, new materials have emerged to meet these requirements [3]. In response to this demand, an emerging technology known as all-solid-state lithium-metal batteries (ASSLMBs) has been adopted, utilizing solid-state electrolytes (SSEs) as well. Besides exhibiting better properties than LIBs, this type of battery enhances the safety of secondary batteries [4]. Additionally, solid-state batteries, with their multiple applications, can be used in electronic components, electric vehicles, and stationary battery storage [5].

The use of lithium cathodes with advanced materials has garnered significant interest, and some research has been conducted on this type of material. For instance, the  $\text{Li}_{1-x}\text{FePO}_4$  cathode, derived from the olivine-type mineral [6], presents low electronic conductivity and a high lithium diffusion barrier [7]. Other materials studied include  $\text{Li}_{1-x}\text{CoO}_2$  and  $\text{Li}_{1-x}\text{MnO}_2$ , structured in [8], [9]. The former has a 2D layered crystalline structure, while the latter has a 3D structure. However, these structures can have some disadvantages. For

\* Corresponding author: [z.zarhri@gmail.com](mailto:z.zarhri@gmail.com)

example,  $\text{Li}_{1-x}\text{CoO}_2$  operates at high cycle rates and, due to the cobalt element, production costs are high and non-renewable [10,11]. The spinel-type  $\text{Li}_{1+x}\text{Mn}_2\text{O}_4$  suffers from irreversible fading during its cycling [12]. In the search for materials for energy storage, a family of antiperovskite dichalcogenides has shown excellent properties. For example, their discharge capacity is  $120 \text{ mA h g}^{-1}$  at  $30 \text{ mA g}^{-1}$ . They also exhibit very good rate capability, with  $270 \text{ mA g}^{-1}$ , and their capacity losses are  $80 \text{ mA h g}^{-1}$  [13,14].

In this work, the structural, optical, and electronic properties of the  $(\text{Li}_{1-x}\text{Fe})_3\text{SO}$  antiperovskite, doped with lithium proportions in the crystalline structure, will be analyzed using first-principles calculations. There are no theoretical analyses of this material in the literature yet, thus complementing previously reported experimental results.

## 2 Computational Method

The WIEN2k computational package was utilized, employing the full-potential linearized augmented plane wave (FP-LAPW) method within Density Functional Theory (DFT) calculations [15]. The exchange-correlation potential used was the Tran and Blaha modified Becke-Johnson (TB-mBJ) potential [16]. Unit cells were created for the compounds  $\text{Li}_3\text{SO}$ ,  $\text{Fe}_3\text{SO}$ , as well as for the Fe-doped compounds  $(\text{Li}_2\text{Fe})\text{SO}$  and  $(\text{LiFe}_2)\text{SO}$ . Additionally, a supercell approximation was used for the compound  $(\text{LiFe}_3)\text{S}_2\text{O}_2$ .

The crystalline solid of the antiperovskite was initially optimized using DFT calculations to obtain the lattice parameters. The optimized structure was then analyzed to calculate various physical properties, such as the density of states (DOS) and electronic band structure. Both calculations were performed using a K-point mesh, and its optical properties were analyzed using the Bethe-Salpeter equation. To verify the accuracy of our DFT calculations, convergence tests were conducted, including energy cut-off, lattice parameters, and K-point density. Additionally, the use of DFT calculations in conjunction with WIEN2k provided a precise and reliable approach to estimate the physical and optoelectronic properties at the quantum level of our studied antiperovskites [17].

Our  $\text{Li}_3\text{SO}$  perovskite has lattice parameters and atomic positions of  $A-C=7.39 \text{ \AA}$  and  $B=14.79 \text{ \AA}$ , with a space group of  $\text{Pm}\bar{3}\text{m}$ , and its structure closely resembles a simple cubic structure. In Figure 1(a), we observe the crystalline structure of the undoped  $\text{Li}_3\text{SO}$  antiperovskite. In Figure 1(b), we observe the structure with Fe atoms doped in the  $\text{Li}_3\text{SO}$  antiperovskite, resulting in  $(\text{Li}_2\text{Fe}_1)\text{SO}$ .

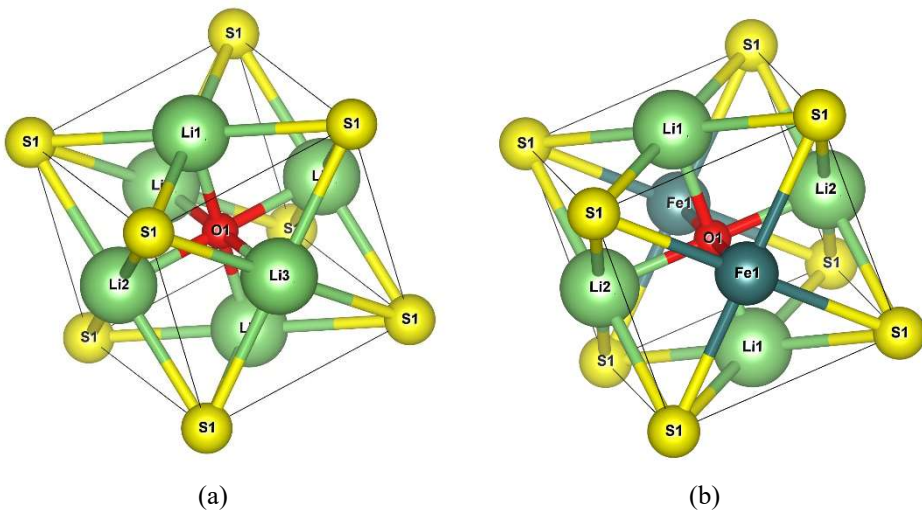


**Fig.1.** (a)  $\text{Li}_3\text{SO}$  structure (b),  $(\text{Li}_2\text{Fe}_1)\text{SO}$  structure

**Table 1.** pore diameter and specific surface area of TiO<sub>2</sub> vs annealing temperature

Annealing temperature (°C)	Pore diameter $P_D$ (nm)	Specific area ( $SBETm^2.g^{-1}$ )
100	1.95	205
300	2.09	160
500	4.86	125

The annealing temperature augments give rise to pores diameter ( $P_D$ ) which reaches the max up to 500 ° C, on the other hand, we noticed a systematic decrease of the specific area ( $SBET$ ) values. So, to keep high  $SBET$ , the annealing temperature is limited to 300 ° C.

### 3 Results and discussion

#### 3.1 Total density of states

In Figure 2, the density of states (DOS) of the Li<sub>3</sub>SO material shows the emergence of new energy levels or states as the atoms transition from Li to Fe. This indicates that the incorporation of Fe atoms into the Li<sub>3</sub>SO material introduces new energy levels into the electronic structure [18]. These additional energy levels may be associated with the electrons from the Fe atoms and could influence the electronic and optical properties of the material, affecting its band structure [19]. This could result in a change in the band gap width, which is the energy difference between the allowed and forbidden levels for electrons. These changes can affect the electrical conductivity and optical properties of the material.

Furthermore, the substitution of Li atoms by Fe affects the ionic mobility within the material, which could have implications for its use in batteries. Ionic mobility is a key factor in rechargeable batteries, as it affects the ability of lithium ions (Li<sup>+</sup>) to move in and out of the material during charge and discharge [20].

The analysis of the DOS and the new energy states can provide insights into the ion intercalation capability of the material. If the new energy states are suitable for the intercalation and deintercalation of lithium ions, this could indicate a higher energy storage capacity in a battery. Additionally, changes in ionic mobility can influence the charge and discharge rates of the battery, which is also relevant for its performance [21].

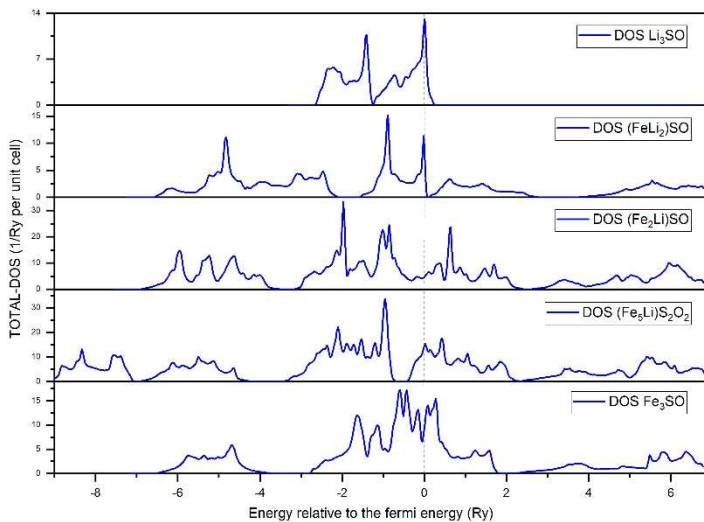


**Fig. 2.** Fe doped Li<sub>3</sub>SO total density of states.

### 3.2 Partial densities of states (PDOS)

The partial density of states (Figure 3) shows a higher contribution of Fe atoms in the new emerging states near the Fermi level due to atomic substitution (gradual replacement of Li with Fe). The presence of Fe atoms in the emerging states suggests the formation of hybrid d bonds between them and the surrounding S atoms. This hybridization can lead to new electronic states with specific energies, indicating a reorganization of the material's electronic structure. Since Fe is known for its magnetic properties, its presence in the new states could introduce magnetic interactions into the  $\text{Li}_3\text{SO}$  material. This could impact conductivity and energy storage capacity, especially in battery systems that rely on magnetic phenomena [22].

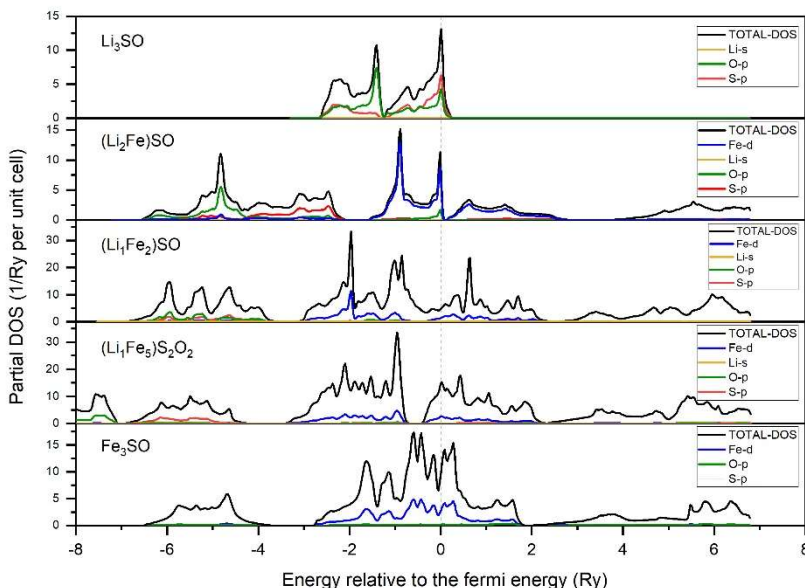


**Fig. 3.** Total and Partial Density of States of Fe-Doped  $\text{Li}_3\text{SO}$  Antiperovskite

The new emerging states may be related to electronic interaction phenomena between Li, S, and Fe atoms. This can involve charge transfer, electronic polarization, or changes in the energy bands of the material. Such phenomena could lead to the emergence of new states near the Fermi level and affect the material's electronic conductivity. This impacts electron mobility, their ability to carry electrical current, and their involvement in redox reactions during battery charging and discharging, which significantly influences the electronic properties of the material and its capability to intercalate and deintercalate lithium ions during battery operation [21].

If the new emerging states near the Fermi level facilitate greater intercalation of lithium ions, this could enhance the energy storage capacity of the battery. Additionally, if the new states improve electron mobility, this could lead to higher electronic conductivity in the battery, thereby improving its efficiency and performance.

### 3.3 Optical properties

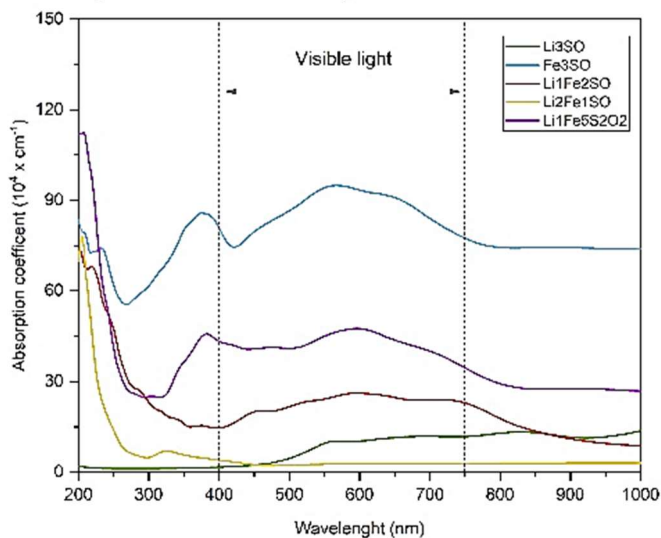
Figure 4(a) presents the results of the variation in the absorption coefficient as a function of wavelength for  $\text{Li}_3\text{SO}$  material with gradual atomic substitution, with Fe replacing Li sites.

The graph indicates that the  $\text{Li}_3\text{SO}$  material has a low light absorption capacity up to 500 nm, but beyond this wavelength, it shows an increase in absorption capacity, reaching a constant value of 20% at higher wavelengths. As the substitution of Li atoms with Fe in the  $\text{Li}_3\text{SO}$  material increases, the absorption coefficient also increases. This means that the resulting material with a higher proportion of Fe has a greater capacity to absorb light compared to the original material, which primarily contains Li atoms.

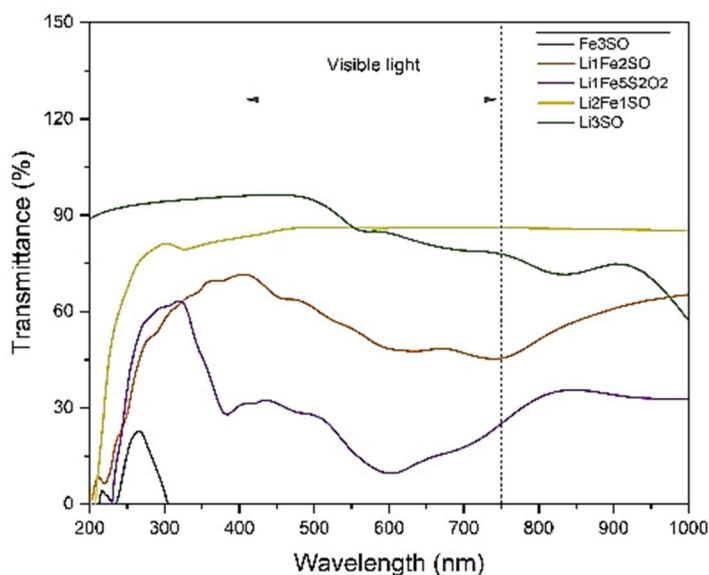
This effect may be caused by electronic transition phenomena, where the substitution of Li atoms with Fe can alter the electronic structure of the material. Electrons in Fe atoms may have energy levels in the visible or near-visible spectrum region, resulting in a higher light absorption capacity at those specific wavelengths [23].

Additionally, the substitution of Li atoms with Fe may lead to changes in the crystalline structure of the material. These changes can affect how light interacts with the material, such as diffraction, reflection, and absorption, which would be reflected in an increased absorption coefficient.

Therefore, the incorporation of Fe atoms into the  $\text{Li}_3\text{SO}$  material may introduce impurities or defects into the crystalline structure. These defects can act as centers for additional light absorption, contributing to the increased absorption coefficient.



(a)



(b)

**Fig. 4.** Optical Parameters Calculated (a), Absorption Coefficient (b) Transmittance

Figure 4(b) presents the transmittance of the same material, and it can be observed that the transmittance decreases as Li atoms are gradually replaced with Fe. The decrease in transmittance could be related to the phenomenon of band gap widening as Li atoms are substituted with Fe. This implies that the material becomes less transparent at certain wavelengths, resulting in lower light transmittance through the material [24].

Additionally, the introduction of Fe atoms into the material may lead to the emergence of additional energy levels in the electronic structure. These energy levels can result in selective light absorption at certain wavelengths, thereby decreasing transmittance in those specific regions of the spectrum. Thus, the gradual substitution of Li atoms with Fe affects the crystalline structure of the  $\text{Li}_3\text{SO}$  material, altering how light interacts with the material, such as through scattering or reflection, which can in turn reduce transmittance.

## 4 Conclusion

The gradual substitution of Li atoms with Fe in  $\text{Li}_3\text{SO}$  material can have a significant impact on its optical properties, density of states, and potential applications in batteries. The emergence of new energy states, especially involving Fe and S atoms, suggests a reorganization of the electronic structure and possible electronic interactions within the material. These changes influence the lithium ion intercalation capability, electronic conductivity, and energy storage capacity in a battery. New energy states near the Fermi level could indicate an increase in energy storage capacity, while the greater contribution of Fe atoms to these new states could affect electronic conductivity and ion mobility, generating new interactions within the material.

Sulfur is known for its high theoretical lithium storage capacity, which could translate into a high specific capacity for the battery. However, the actual capacity and stability of a sulfur electrode may be limited by challenges such as volumetric expansion during charge

and discharge cycles. Nonetheless, good electrochemical stability of the material can prevent undesirable reactions and degradation.

**Acknowledgements:** The authors would like to thank CONAHCYT Mexico for all support.

## References

1. H. Chen, T. N. Cong, W. Yang, C. Tan, Y. Li, Y. Ding, Progress in electrical energy storage system: A critical review. *Prog. Nat. Sci.* 19, 291–312 (2009). <https://doi.org/10.1016/j.pnsc.2008.07.014>
2. J.-M. Tarascon, M. Armand, Issues and challenges facing rechargeable lithium batteries. *Nature* 414, 359–367 (2001). <https://doi.org/10.1038/35104644>
3. V. Etacheri, R. Marom, R. Elazari, G. Salitra, D. Aurbach, Challenges in the development of advanced Li-ion batteries: a review. *Energy Environ. Sci.* 4, 3243 (2011). <https://doi.org/10.1039/c1ee01598b>
4. A. Manthiram, X. Yu, S. Wang, Lithium battery chemistries enabled by solid-state electrolytes. *Nat. Rev. Mater.* 2, 16103 (2017). <https://doi.org/10.1038/natrevmats.2016.103>
5. Y. Liang et al., A review of rechargeable batteries for portable electronic devices. *InfoMat* 1, 6–32 (2019). <https://doi.org/10.1002/inf2.12000>
6. A. K. Padhi, K. S. Nanjundaswamy, J. B. Goodenough, Phospho-olivines as positive-electrode materials for rechargeable lithium batteries. *J. Electrochem. Soc.* 144, 1188–1194 (1997). <https://doi.org/10.1149/1.1837571>
7. W.-J. Zhang, Structure and performance of LiFePO<sub>4</sub> cathode materials: A review. *J. Power Sources* 196, 2962–2970 (2011). <https://doi.org/10.1016/j.jpowsour.2010.11.113>
8. A. R. Armstrong, P. G. Bruce, Synthesis of layered LiMnO<sub>2</sub> as an electrode for rechargeable lithium batteries. *Nature* 381, 499–500 (1996). <https://doi.org/10.1038/381499a0>
9. K. Mizushima, P. C. Jones, P. J. Wiseman, J. B. Goodenough, Li<sub>x</sub>CoO<sub>2</sub> (0 < x < 1): A new cathode material for batteries of high energy density. *Mater. Res. Bull.* 15, 783–789 (1980). [https://doi.org/10.1016/0025-5408\(80\)90012-4](https://doi.org/10.1016/0025-5408(80)90012-4)
10. R. Marom, S. F. Amalraj, N. Leifer, D. Jacob, D. Aurbach, A review of advanced and practical lithium battery materials. *J. Mater. Chem.* 21, 9938 (2011). <https://doi.org/10.1039/c0jm04225k>
11. M. S. Whittingham, Lithium batteries and cathode materials. *Chem. Rev.* 104, 4271–4302 (2004). <https://doi.org/10.1021/cr020731c>
12. M. M. Thackeray, W. I. F. David, P. G. Bruce, J. B. Goodenough, Lithium insertion into manganese spinels. *Mater. Res. Bull.* 18, 461–472 (1983). [https://doi.org/10.1016/0025-5408\(83\)90138-1](https://doi.org/10.1016/0025-5408(83)90138-1)
13. K. T. Lai, I. Antonyshyn, Y. Prots, M. Valldor, Anti-perovskite Li-battery cathode materials. *J. Am. Chem. Soc.* 139, 9645–9649 (2017). <https://doi.org/10.1021/jacs.7b04444>
14. D. Mikhailova et al., Operando studies of antiperovskite lithium battery cathode material (Li<sub>2</sub>Fe)SO. *ACS Appl. Energy Mater.* 1, 6593–6599 (2018). <https://doi.org/10.1021/acsaem.8b01493>

15. P. Blaha, K. Schwarz, P. Sorantin, S. B. Trickey, Full-potential, linearized augmented plane wave programs for crystalline systems. *Comput. Phys. Commun.* 59, 399–415 (1990). [https://doi.org/10.1016/0010-4655\(90\)90187-6](https://doi.org/10.1016/0010-4655(90)90187-6)
16. F. Tran, P. Blaha, Accurate band gaps of semiconductors and insulators with a semilocal exchange-correlation potential. *Phys. Rev. Lett.* 102, 226401 (2009). <https://doi.org/10.1103/PhysRevLett.102.226401>
17. Z. Lu, F. Ciucci, Anti-perovskite cathodes for lithium batteries. *J. Mater. Chem. A* 6, 5185–5192 (2018). <https://doi.org/10.1039/C7TA11074J>
18. Z. Zarhri, Y. Ziat, O. El Rhazouani, A. Benyoussef, A. Elkenz, Titanium atoms dimerization phenomenon and magnetic properties of titanium-antisite (TiO) and chromium doped rutile TiO<sub>2</sub>, ab-initio calculation. *J. Phys. Chem. Solids* 94, 12–16 (2016). <https://doi.org/10.1016/j.jpcs.2016.03.002>
19. N. Xin et al., Improving the thermoelectric performance of Cu-doped MoS<sub>2</sub> film by band structure modification and microstructural regulation. *Appl. Surf. Sci.* 611, 155611 (2023). <https://doi.org/10.1016/j.apsusc.2022.155611>
20. Y. Li et al., Intrinsic electron mobility and lattice thermal conductivity of  $\beta$ -Si<sub>3</sub>N<sub>4</sub> from first-principles. *Solid State Commun.* 361, 115066 (2023). <https://doi.org/10.1016/j.ssc.2023.115066>
21. X.-M. Zheng et al., Superior Li storage anode based on novel Fe-Sn-P alloy prepared by electroplating. *Electrochim. Acta* 247, 314–320 (2017). <https://doi.org/10.1016/j.electacta.2017.07.002>
22. M. A. M. M. Al-samet, E. Burgaz, Improving the lithium-ion diffusion and electrical conductivity of LiFePO<sub>4</sub> cathode material by doping magnesium and multi-walled carbon nanotubes. *J. Alloys Compd.* 947, 169680 (2023). <https://doi.org/10.1016/j.jallcom.2023.169680>
23. Y. Da, J. Zhou, Microscopic mechanisms of Mn-doped CaCO<sub>3</sub> heat carrier with enhanced optical absorption and accelerated decomposition kinetics for directly storing solar energy. *Sol. Energy Mater. Sol. Cells* 250, 112103 (2023). <https://doi.org/10.1016/j.solmat.2022.112103>
24. S. Han et al., Modification of the band gap of Ruddlesden–Popper perovskites Sr<sub>n+1</sub>Ti<sub>n</sub>O<sub>3n+1</sub> (n=1, 2, 3, and  $\infty$ ) by Fe ion irradiation doping. *Ceram. Int.* 49, 7396–7403 (2023). <https://doi.org/10.1016/j.ceramint.2022.10.209>